Free Energy Control of Reaction Pathways in Electrogenerated Chemiluminescence

Ernest L. Ritchie,[†] Paolo Pastore,[‡] and R. Mark Wightman*[,†]

Contribution from the Department of Chemistry, University of North Carolina, Chapel Hill, North Carolina 27599-3290, and Dipartimento di Chimica Inorganica, Metallorganica e Analitica, Universita di Padova, Via Marzolo 1, 35131 Padova, Italy

Received May 12, 1997. Revised Manuscript Received July 28, 1997[⊗]

Abstract: Electrogenerated chemiluminescence (ECL) from 9,10-diphenylanthracene (DPA) in acetonitrile has been examined following reaction of its radical ions with various donors and acceptors by using high speed potential pulses at a microelectrode. The reaction pathways were identified by examining the reaction orders of the limiting reagents and by comparison of the temporal emission pulses with simulated reaction schemes. For reactions with a free energy value more negative than that required to directly form the excited state singlet (3.06 eV), first-order behavior was observed for DPA radical ions indicating direct singlet formation (S-route). For the remaining systems the reaction order was second order in DPA radical ions, indicative of excited singlet formation via triplet−triplet annihilation (T-route). Despite evidence of triplet quenching by the unreacted radical ions, the efficiency of photon production at high concentrations of DPA by the T-route (0.012) approached that of the S-route, and is much higher than previously reported. For $DPA^{\bullet+}$ and naphthyl phenyl ketone a mixed reaction order was found. The free energy of this reaction is deficient by 0.05 eV, and in this case, direct singlet formation is able to compete with the more energetically favorable triplet pathway. The high efficiency experimentally found for the T-route suggests that it may be an alternate scheme to employ in solid-state display devices.

Introduction

Electrogenerated chemiluminescence (ECL), the production of light from intermediates generated during electrolysis,[1,2] occurs when the energy liberated by chemical reactions is sufficient to generate a species in an electronically excited form. This phenomenon has long been of interest since it provides a simple route for photon production. Excited state formation in such reactions is a consequence of the Marcus prediction that formation of the ground state is sufficiently exothermic that it lies in an inverted kinetic region.[3] This has been demonstrated in investigations of the effect of free energy on the routes of electron transfer reactions resulting in ECL,[4] and used to predict variations in the observed ECL efficiencies.[5] The efficient nature of ECL, coupled with the simplicity of photonic detection, has led to its use in trace analytical methods, with subpicomolar detection limits reported in some applications.[6]

Recently, there has emerged a renewed interest in the mechanisms of ECL production driven by the development of electrochemically based display devices formed in solid-state polymeric and molecular films.[7−9] In many respects, light generation from these devices appears to follow the classical pathways identified for ECL generation in solution. The devices exhibit delays in light production, have limiting currents consistent with diffusional mass transport, and emit light equivalently under forward and reverse bias—all features that are unlike solid-state diodes. Furthermore, the emission occurs with potential biases sufficient to generate the appropriate redox species as in solution. Thus, it has become important to quantitatively evaluate pathways that lead to ECL to identify potential molecular candidates for the design of more efficient solid-state devices.

ECL reactions that involve radical anions and cations have classically been shown to follow two distinct pathways.[1,2] Electrochemically produced radical ions, an electron donor ($D^{\bullet-}$) and an electron acceptor ($A^{\bullet+}$, reactions 1 and 2 below), formed from parent molecules A and D, diffuse together to form an encounter complex. Such a complex can decompose via electron transfer to form an emitting excited singlet state ($^1A^*$) or a nonemitting excited triplet state ($^3A^*$) as shown in reaction 3. The former path has traditionally been referred to as the S-route.[2] (The rate for formation of the ground state of the parent compounds lies in the Marcus inverted region and can

* To whom correspondence should be addressed.
† University of North Carolina.
‡ Universita di Padova.
⊗ Abstract published in *Advance ACS Abstracts,* December 1, 1997.

(1) (a) Knight, A. W.; Greenway, G. M. *Analyst* **1994**, *119*, 879−890. (b) Faulkner, L. R. *Int. Rev. Sci.: Phys. Chem. Ser. Two* **1975**, *9*, 213−263.
(2) Faulkner, L. R.; Bard, A. J. *Electroanalytical Chemistry*; Marcel Dekker: New York, Vol. 10, 1977; pp 1−95.
(3) Sutin, N. *Acc. Chem. Res.* **1982**, *15*, 275−282.
(4) (a) Tachikawa, H.; Bard, A. J. *Chem. Phys. Lett.* **1974**, *26*, 246−251. (b) Wallace, W. L.; Bard, A. J. *J. Phys. Chem.* **1979**, *83*, 1350−1357. (c) Kapturkiewicz, A. *Chem. Phys.* **1992**, *166*, 259−273.
(5) (a) Maness, K. M.; Wightman, R. M. *J. Electroanal. Chem.* **1995**, *396*, 85−95. (b) Maness, K. M.; Bartelt, J. E.; Wightman, R. M. *J. Phys. Chem.* **1994**, *98*, 3993−3998. (c) Collinson, M. M.; Wightman, R. M.; Pastore, P. *J. Phys. Chem.* **1994**, *98*, 11942−11947.
(6) (a) Knight, A. W.; Greenway, G. M. *Anal. Commun.* **1996**, *33*, 171−174. (b) Skotty, D. R.; Lee, W.-Y.; Nieman, T. A. *Anal. Chem.* **1996**, *68*, 1530−1535. (c) Xu, X.-H.; Bard, A. J. *J. Am. Chem. Soc.* **1995**, *117*, 2627−2631. (d) Collinson, M. M.; Wightman, R. M. *Science* **1995**, *268*, 1883−1885. (e) Leland, J. K.; Powell, M. J. *J. Electrochem. Soc.* **1990**, *137*, 3127−3131. (f) Ege, D.; Becker, W. G.; Bard, A. J. *Anal. Chem.* **1984**, *56*, 2413−2417.
(7) (a) Maness, K. M.; Terrill, R. H.; Meyer, T. J.; Murray, R. W.; Wightman, R. M. *J. Am. Chem. Soc.* **1996**, *118*, 10609−10616. (b) Maness, K. M.; Masui, H.; Wightman, R. M.; Murray, R. W. *J. Am. Chem. Soc.* **1997**, *119*, 3987−3993.
(8) (a) Pei, Q.; Yang, Y.; Yu, G.; Zhang, C.; Heeger, A. J. *J. Am. Chem. Soc.* **1996**, *118*, 3922−3929. (b) Pei, Q.; Yu, G.; Zhang, C.; Yang, Y.; Heeger, A. J. *Science* **1995**, *269*, 1086−1088.
(9) (a) Sheats, J. R.; Antoniadis, H.; Hueschen, M.; Leonard, W.; Miller, J.; Moon, R.; Roitman, D.; Stocking, A. *Science* **1996**, *273*, 884−888. (b) Kido, J.; Kimura, M.; Nagai, K. *Science* **1995**, *267*, 1332−1334. (c) Clery, D. *Science* **1994**, *263*, 1700−1702.

S0002-7863(97)01537-0 CCC: $14.00

$$A - e^- \rightarrow A^{\bullet +} \quad (1)$$

$$D + e^- \rightarrow D^{\bullet -} \quad (2)$$

$$A^{\bullet +} + D^{\bullet -} \xrightarrow{k_s} {}^1A^* + D$$

$$\xrightarrow[k_t]{} {}^3A^* + D \quad (3)$$

$${}^1A^* \rightarrow A + h\nu \quad (4)$$

be ignored.[4,10]) In previous work we have shown that this reaction scheme satisfactorily accounts for the experimental observations for the case where 9,10-diphenylanthracene plays the role of both A and D.[5,11] Thus, the efficiency of light production (ϕ_{ecl}) is given by:

$$\phi_{ecl} = k_s/(k_s + 3k_t) \quad (5)$$

The numerical factor [3] accounts for the statistics of spin−spin recombination and, for the case where DPA serves as both A and D, k_t is at the diffusion controlled limit.[5,11] In acetonitrile, ϕ_{ecl} for this case is 0.061.[5]

An alternate route to form the excited state singlet is via triplet−triplet annihilation (TTA), commonly referred to as the T-route.[12] In this case, two excited state triplets diffuse together with energy transfer resulting in an excited state singlet and a ground state molecule (reaction 6), with a rate constant given by k_{tta}:

$$2\,{}^3A^* \xrightarrow{k_{tta}} {}^1A^* + A \quad (6)$$

This pathway is the predominant one leading to singlet emission in ECL systems that do not have sufficient energy to populate the excited singlet state directly.[13,14] Reported efficiencies for the T-route are generally an order of magnitude smaller than those for the S-route.[13] These low efficiencies are not predicted from Marcus theory and spin−spin statistics.[2] Formation of excited triplet states will occur rapidly and without competition (reaction 3), and statistically $^1/_9$ of the reactions of two triplets (reaction 6) would be predicted to lead directly to singlet production.[16] Thus, in the absence of other reactions and taking into account that two DPA ions are required to form a singlet, an efficiency for this pathway of 0.055 would be predicted for DPA, equivalent to that experimentally determined for the S-route. While quenching of triplet states may lower the efficiency,[4,13] this pathway is attractive because it requires less input energy than the S-route.

In this work we have quantitatively reexamined the emission generated from DPA singlets formed during ECL to reveal the operant pathways. To accomplish this, the reaction order of DPA during ECL generation was determined with reactants having different oxidation and reduction potentials. In this way the specific pathway and rates could be altered. Inspection of the reaction sequences shows that if the concentration of D is sufficiently large relative to that of A, the reaction will exhibit first-order behavior in A for the S-route. Alternatively, if emission arises from the T-route, then second-order behavior in A will be found. The studies were done in a flow-injection apparatus containing a microelectrode that allows a range of concentrations of reactants to be examined.[11] The microelectrode allows high-frequency potential programs to be employed, minimizing the effects of competing, light-quenching reactions. The data show that formation of the singlet via the T-route is more efficient than previously recognized. Furthermore, by identification of the relevant competing pathways, predictions for optimum light emission can be made. The most efficient conditions for T-route production are found to be at high concentrations. Thus, while T-route ECL is unlikely to be useful for trace analytical schemes, it could be useful in ECL light-emitting devices.

Experimental Section

Apparatus. The flow-injection analysis (FIA) system used was identical with that previously described.[11] A stainless steel syringe pump (ISCO) delivered solvent through a pneumatically controlled valve (SSI) with a 1 mL loop to a channel-type electrochemical cell. The base of the cell was made of epoxy and contained the electrodes. The thickness of the cell was established with a 150 μm thick polyethylene gasket. The cell top was stainless steel and contained a glass window in which a Hamamatsu R5600P photomultiplier tube (PMT) was placed directly across from the working electrode and approximately 4 mm from the glass surface. The PMT was operated at −800 V (John Fluke, Model 412A). Its output was directed to a preamplifier (EGG Ortec VT120A) and multichannel scaler (MCS, EGG Ortec T-914) with the discriminator level set at −300 mV. For solutions that gave high light fluxes (>2 × 10^6 CPS (counts per second)), neutral density filters (Melles Griot, 0.5 or 2.0 optical density) were placed between the PMT and cell window to prevent pulse pile-up.

The cell potential was controlled with an arbitrary waveform generator used with HP 34811A Benchlink/Arb software (Hewlett Packard 33120A). The working electrode was connected to a fast current to voltage converter made in-house with gain settings of 5 × 10^5 or 1.25 × 10^7 V/A. A digital oscilloscope (LeCroy 9450) was used to monitor the applied waveforms and collect averaged cyclic voltammograms (100 signals).

Electrode Preparation. Band electrodes (3 μm nominal thickness) were prepared by sandwiching a piece of gold foil (Goodfellow) between two glass spacers (∼100 μm thick) surrounded by two silver counter electrodes (Alfa Aesar, 0.5 mm thickness) that were connected together and served as a quasireference electrode. The layers were joined with epoxy (EPON 828 with 14% metaphenylenediamine, Miller Stephenson) that was cured for 2 h each at 75 and 150 °C. This assembly was placed in a mold and potted in epoxy to form a rectangular structure that formed the floor of the flow injection channel. Disk electrodes were made as previously described.[11] The surface containing the electrodes was polished with sandpaper (300 grit) until the electrodes were exposed. Subsequent polishing was with 400, 600, 1000, and 1500 grit sandpaper followed by 6- and 1-μm diamond paste on Nylon cloths (Buehler). Prior to each experiment, electrodes were polished with 1-μm diamond paste, rinsed with acetone, and wiped dry with a Kimwipe (Kimberly-Clark).

Procedures. Acetonitrile was delivered from the pump to the electrochemical cell at a flow rate of 200 μL/min. The loop injector was used to introduce reagents to the electrode in acetonitrile containing 0.1 M tetrabutylammonium hexafluorophosphate (TBAH) and deoxygenated with N_2. Normally the concentration of DPA was varied while the concentration of the donor or acceptor remained constant at 1 mM. The potential waveform was a continuous, 1 kHz square wave with potential limits between 100 and 200 mV beyond the $E_{1/2}$ values of the redox couples as determined from cyclic voltammograms so that the production of ECL reagents was diffusion limited. Solutions were successively injected from lowest to highest DPA concentration to limit cross contamination. PMT counts were binned at 100 kHz for 2 complete cycles of the square wave and the sum of 1000 responses was obtained (2 s total).

(10) (a) Gould, I. R.; Farid, S. *Acc. Chem. Res.* **1996**, *29*, 522−528.
(11) Collinson, M. M.; Wightman, R. M. *Anal. Chem.* **1993**, *65*, 2576−2582.
(12) (a) Visco, R. E.; Chandross, E. A. *Electrochim. Acta* **1968**, *13*, 1187−1196. (b) Feldberg, S. W. *J. Phys. Chem.* **1966**, *70*, 3928−3930.
(13) Beldeman, F. E.; Hercules, D. M. *J. Phys. Chem.* **1979**, *83*, 2203−2209.
(14) (a) Kim, J.; Faulkner, L. R. *J. Am. Chem. Soc.* **1988**, *110*, 112−119. (b) Kapturkiewicz, A. *J. Electroanal. Chem.* **1994**, *372*, 101−116.
(15) Saltiel, J.; Atwater, B. W. *Adv. Photochem.* **1988**, *14*, 1−85.
(16) Hoytink, G. J. *Acc. Chem. Res.* **1969**, *2*, 114−120.

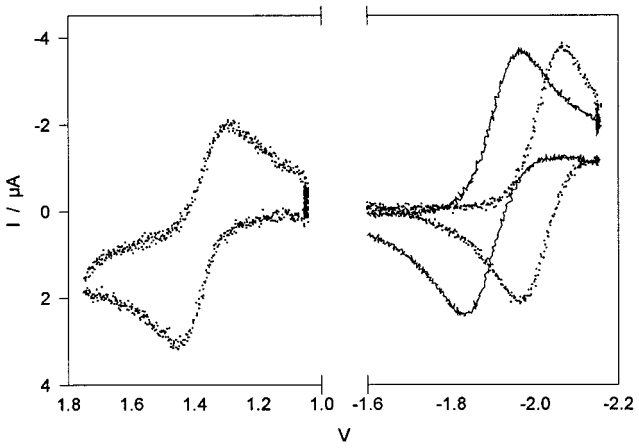

Figure 1. Background subtracted cyclic voltammograms of 1 mM 9,10-diphenylanthracene (DPA, dotted lines) and of 1 mM benzophenone (BP, solid line) in ACN containing 0.1 M tetrabutylammonium hexafluorophosphate (TBAH). The electrode was an Au band electrode (3 μm thick) used at a scan rate of 2 kV/s.

Finite Difference Simulation. The reactions described in steps 3, 4, and 6 above were simulated by the finite difference procedure employing the hopscotch algorithm. The simulation was identical with that published previously[17] except it was modified to account for different concentrations of $A^{\bullet-}$ and $D^{\bullet+}$ and to allow the T-route to occur. The simulation is based on semiinfinite linear diffusion and, thus, only approximates the fluxes generated with the band electrode where some convergent diffusion will occur with the potential frequency employed. The simulations shown are from the fifth cycle of a continuous square wave and are taken as the steady-state response. To account for the finite rise time of the microelectrode to potential steps, the solution resistance and double layer capacitance were included.

The input variables were the step times, the concentration of A and D, the E°'s and step potentials, the diffusion coefficient ($D_{DPA} = 1.3 \times 10^{-5}$ cm^2 s^{-1} in acetonitrile[5c] was used for all species), and the rate constants. All simulations employed a heterogeneous rate constant of 1 cm s^{-1} with a charge transfer coefficient of 0.5. These values are consistent with those experimentally determined at microelectrodes for aromatic hydrocarbons.[17] Agreement of the simulated curves with the experimental data is based on normalized amplitudes. Unless otherwise indicated the S-route simulations employed a k_{annih} ($=k_s + 3k_t$) value of 2×10^{10} M^{-1} s^{-1}, the value previously reported to be the best fit for ECL from the $DPA^{\bullet+}/DPA^{\bullet-}$ system.[5c] This value is the computed diffusion controlled rate constant in acetonitrile. For the T-route simulation the following values were employed: $k_s = 0$ and $k_t = 1 \times 10^{10}$ M^{-1} s^{-1} with k_{tta} and k_q adjusted to fit the shape of the experimental curves. The number of nodes in the space-time grid of the simulation was computed based on the value of the largest value of λ ($\lambda = ktc$, where k is the largest second-order rate constant in the reaction sequence, t is the experimental time, and c is the concentration of the highest reactant) as previously described.[17]

Reagents. Acetonitrile (ACN, UV, Burdick & Jackson), 2-benzoylnaphthalene (or naphthyl phenyl ketone, NPK, Aldrich), benzil (Aldrich), benzophenone (BP, Aldrich), 4-methoxybenzophenone (MOBP, Aldrich), 4-methylbenzophenone (MBP, Aldrich), and 9-fluorenone (9-F, Aldrich) were used as received. *N*,*N*,*N*′,*N*′-Tetramethyl-1,4-phenylenediamine (TMPD, Aldrich) was purified by vacuum sublimation. 9,10-Diphenylanthracene (DPA, Aldrich) was recrystallized twice from absolute ethanol. TBAH (Aldrich) was recrystallized from 95% ethanol.

Results

Energy Sufficient System. A cyclic voltammogram of equimolar solutions of DPA and BP reveals three reversible couples (Figure 1). BP is reduced at slightly more positive potentials than DPA, and is not oxidized in the potential range examined. Values of $E_{1/2}$ obtained from such curves were used to compute the differences in free energy summarized in Table 1. With the energy of the excited state singlet[13] and triplet[19] of DPA, 3.06 and 1.8 eV, respectively, the free energy of the reaction between $BP^{\bullet-}/DPA^{\bullet+}$ can be calculated. It is clear from the values summarized in Table 1 that this system is energy sufficient for direct formation of the DPA excited singlet.

Table 1. Reaction Energies of DPA with Various Donors/Acceptors and the Reaction Order (Slope) from the Solid Lines in Figure 3

compd	$\Delta E_{1/2}$ (V)	reaction order (slope)
BP	3.15	0.96
MBP	3.24	0.99
MOBP	3.24	0.99
NPK	3.01	1.27
TMPD	2.15	1.98
9-F	2.60	1.98
benzil	2.41	1.97

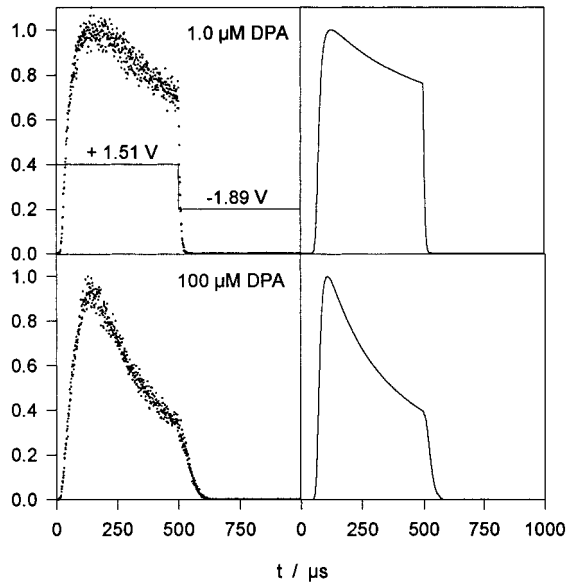

Figure 2. Normalized ECL seen for an energy sufficient system. Left panels: ECL generated in ACN containing 0.1 M TBAH, 1.0 (upper) and 100 μM (lower) DPA, and 1.0 mM BP. Right panels: The corresponding simulated curves employing $k_{annih} = 2 \times 10^{10}$ M^{-1} s^{-1}. The potential steps employed are superimposed on the experimental data.

The ECL obtained from DPA with 1 mM BP during a single cycle of the potential program is shown in Figure 2 for DPA at two different concentrations. In both cases, the majority of the photons are observed during the positive potential step where $DPA^{\bullet+}$, the limiting reagent, is formed ($t > 0$ μs). During this step, the rate of photon emission rises quickly to a maximum following application of the potential, and then decays. Finite-difference simulation of energy sufficient systems (Figure 2, right column) shows similar temporal profiles for photon emission at both concentrations. The finite time to reach a maximum is due to the time constant of the electrochemical cell, which is accounted for in the simulation. The subsequent decrease is due to movement of the reaction zone, the location where the influx of anions generated on the previous step encounters the outward flux of cations, away from the electrode surface. The rate of emission decay is slower with lower concentrations of DPA because control of the rate of photon production has evolved from diffusional mass transport to the rate of annihilation. The transient light production at the

(17) Pastore, P.; Magno, F.; Collinson, M. M.; Wightman, R. M. *J. Electroanal. Chem.* **1995**, *397*, 19−26.

(18) Howell, J. O.; Wightman, R. M. *Anal. Chem.* **1984**, *56*, 524−529.

(19) Brinen, J. S.; Koren, J. G. *Chem. Phys. Lett.* **1968**, *2*, 671−672.

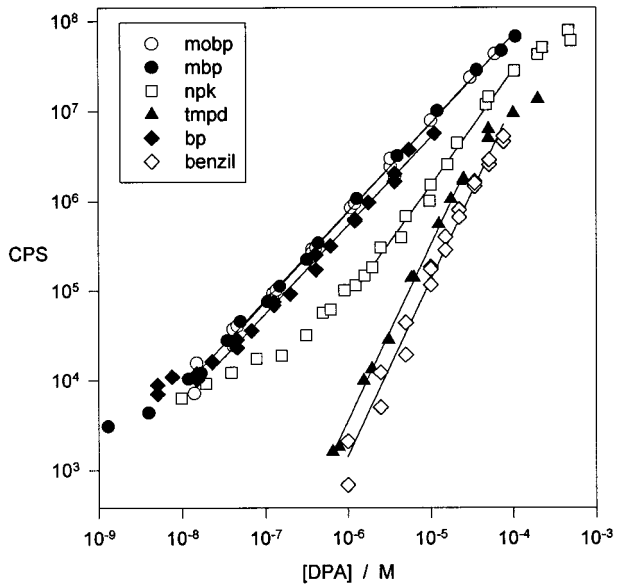

Figure 3. Logarithmic plot of ECL obtained in ACN containing 0.1 M TBAH versus DPA concentration. For each curve, the reagents indicated by the symbols were used as donor or acceptor at 1.0 mM concentration. The slopes of the best fit lines are given in Table 1.

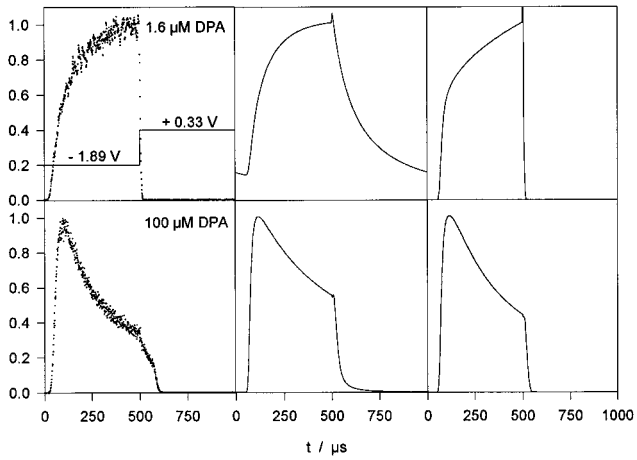

Figure 4. Normalized ECL seen for energy deficient systems. Left panels: ECL generated in ACN containing 0.1 M TBAH, 1.6 (upper) and 100 μM (lower) DPA, and 1.0 mM TMPD. The potential steps employed are superimposed on the experimental data. Center panels: simulated curves for ECL for the conditions in the left panels without quenching ($k_s = 0$, $k_t = 10^{10}$ M^{-1} s^{-1}, $k_{tta} = 2 \times 10^9$ M^{-1} s^{-1}). Right panels: Simulated curves identical with the center panels except a quenching step by radical ions of DPA$^{\bullet-}$ and TMPD$^{\bullet+}$ has been included ($k_q = 10^{10}$ M^{-1} s^{-1}).

beginning of the negative going step ($t > 500$ μs) is due to the presence of residual DPA$^{\bullet+}$ not reduced by the electrode.

Reaction Orders. For all of the donors and acceptors (held at 1 mM concentration) summarized in Table 1, the reaction order in DPA and its intermediates was examined by varying the concentration of DPA over two or more orders of magnitude. For each of the reaction pairs, prior work has shown that the emitting state is the DPA excited singlet, although excited triplet states of some of the other species are energetically accessible.[13] The results are shown in logarithmic form in Figure 3, and the respective slopes are given in Table 1 (for a DPA concentration greater than 100 μM a negative deviation from linearity occurs because the assumption of pseudo-zero-order behavior in the higher concentration species is no longer true). For all of the compounds that are energy sufficient, a linear slope of approximately 1 is obtained, the behavior expected for direct formation of the excited singlet state. The reaction order for ECL with NPK as the higher concentration reagent appears to alter with concentration. At low DPA concentrations (between 100 nM and 1 μM), unity slope is found, whereas the slope increases as the concentration is raised. In the intermediate region the best-fit slope is non-integer ($m = 1.27$), indicative of competing mechanisms.

The chemical systems with insufficient energy to directly form the excited state singlet have a slope of approximately 2 (Table 1) indicating the presence of a second-order, rate-limiting step, i.e. formation of the excited state singlet via the T-route. At high concentrations of DPA relative to the donor or acceptor, the curves for S- and T-route emission approach one another. For example, the TMPD$^{\bullet+}$/DPA$^{\bullet-}$ system provides 18% of the light seen for the DPA$^{\bullet+}$/MOBP$^{\bullet-}$ system at the higher concentrations whereas at lower concentrations the two systems differ in photon production by two orders of magnitude (Figure 3). The DPA$^{\bullet+}$/MOBP$^{\bullet-}$ system has the same efficiency as the DPA$^{\bullet+}$/DPA$^{\bullet-}$ reaction in acetonitrile (also an S-route system).[13] Taking this value to be 0.061, the value we measured in acetonitrile,[5b] the T-route efficiency observed at high concentration is 0.012. While this is lower than predicted in the absence of triplet quenching, it is significantly greater than the highest values previously reported.[13,20]

Simulation of the T-route was done for multiple concentrations, and a plot was constructed in the same fashion as Figure 3. The slope of the resulting line was 1.98. In contrast simulations of the S-route led to a plot with a slope of 0.99. In both cases the correlation coefficients were greater than 0.999.

Time Dependence of an Energy Deficient System. The light produced by the reaction of the TMPD$^{\bullet+}$ and DPA$^{\bullet-}$ system has the characteristics of the excited singlet state of DPA.[20] However, thermodynamic parameters obtained from cyclic voltammetry (Table 1) show that this system is energy deficient with respect to direct formation of the excited singlet state although the excited triplet is energetically accessible. The time course of the ECL obtained with 1 mM TMPD during one cycle of the potential program is shown in Figure 4 for DPA at two different concentrations. At the higher DPA concentration, photon emission occurs during the negative going step ($t > 0$) and is similar to that seen for S-route cases, indicative of control by diffusional mass transport. At lower DPA concentrations, however, while the photon emission occurs during the same step, the photon flux increases during the potential step. In both cases, no light is observed on the positive step after the residual DPA$^{\bullet-}$ has reacted. Thus, the data in Figure 3 and the nature of the time course of light evolution for energy deficient systems both differ from that found for S-route systems, and are entirely consistent with the second-order behavior in DPA radical ions expected for the T-route.

Simulation of the energy deficient case (Figure 4, center), accounting for reactions 1−4 and 6, shows behavior similar to the experimental data during the negative potential step.[22] It predicts a maximum as is observed at high DPA concentration and the continued growth of emission at low DPA concentration. On the other step ($t > 500$ μs), however, the simulation with these conditions does not agree with the experimental data. The simulations predict a continued photon flux during this step arising from the TTA reaction continuing at distances far from

(20) (a) Bezman, R.; Faulkner, L. R. *J. Am. Chem. Soc.* **1972**, *94*, 6331−6337. (b) Bezman, R.; Faulkner, L. R. *J. Am. Chem. Soc.* **1973**, *95*, 3083.

(21) Faulkner, L. R.; Bard, A. J. *J. Am. Chem. Soc.* **1969**, *91*, 209−210.

(22) The value of k_t (10^{10} M^{-1} s^{-1}) was selected to be close to k_d (calculated to be 2×10^{10} M^{-1} s^{-1}).[7] The value of k_{tta}, 2×10^9 M^{-1} s^{-1}, was selected to be approximately $^1/_9$ of k_d.

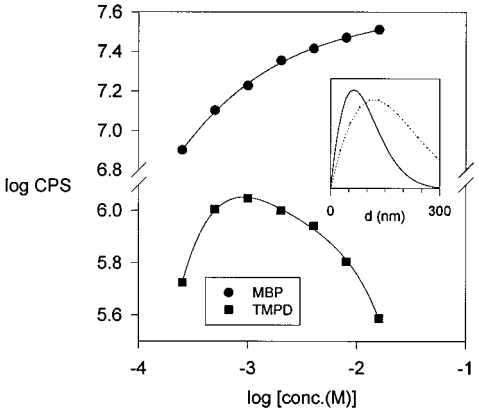

Figure 5. Effect of varying concentration of the nonemitting species. Upper curve: ECL from 20 μM DPA and various [MBP], an energy sufficient system. Lower curve: ECL from 20 μM DPA with various [TMPD], an energy deficient system. Insert: simulated emission profile for solutions containing 8 mM MBP (solid line) and 0.5 mM MBP (dotted line) with 20 μM DPA at $t = 250$ μs.

the electrode. This is due to the long lifetime of the excited triplet (2.5 ms compared to a singlet lifetime of 7.7 ns).[23] Photon absorption by the donor or its radical cation is not the reason for this discrepancy since neither absorb light efficiently[24] at the emission wavelength, 425 nm.[5]

Since paramagnetic species are well-known to quench triplets,[2,13] the effect of the radical ion concentration was examined. As the concentration of TMPD was raised from 0.5 to 2.0 mM (Figure 5), light efficiency increased due to the non-zero-order dependence of the rate of triplet production on $TMPD^{\bullet+}$ concentration. However, at higher concentrations, a decrease in light production occurred, indicating that the radical cation of TMPD quenches triplets before they can react to form a singlet excited state. The decrease was not seen with the energy sufficient system, $MBP^{\bullet-}$ and $DPA^{\bullet+}$. Inclusion of the quenching pathway

$$^3A^* + Q \xrightarrow{k_q} A + Q \qquad (7)$$

in the simulation with rate constant (k_q) close to diffusion control, removed the predicted emission during the positive potential step and improved the agreement with the experimental results (Figure 4), but also reduced the overall predicted emission 20-fold. In the simulation, quenching of the triplet by the DPA radical ion species was also included. Failure to include this step led to an overestimation of the light output at high DPA concentrations.

ECL of DPA in the Presence of NPK. The data in Figure 3 suggest that competitive pathways are operant in the $NPK^{\bullet-}$/$DPA^{\bullet+}$ system. To further probe this, the individual emission curves for this system were examined (Figure 6, similar results were obtained with less negative potential excursions where $DPA^{\bullet-}$ was not formed). At the highest concentrations tested (>100 μM) a maximum is seen in the photon emission consistent with both pathways. However, at intermediate DPA concentrations (20 μM, Figure 6) the time course has the ascending shape characteristic of the T-route. At lower DPA concentrations (<10 μM), the maximum reappears in the time course, consistent with the S-route but not the T-route. With low DPA concentrations, suppression of the T-route is expected

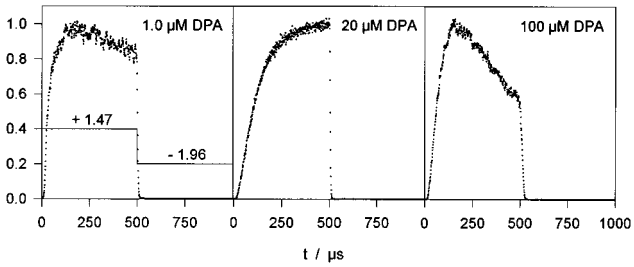

Figure 6. Normalized ECL of the NPK−DPA mixed system for 1, 20, and 100 μM DPA in ACN with 1.0 mM NPK and 0.1 M TBAH at a Au band electrode. The potential steps employed are superimposed on the experimental data. For the 1 μM DPA case, the ECL data resemble that of the singlet mechanism alone (as in Figure 1) due to the low probability of two DPA triplets diffusing together to react. For the 20 μM DPA, the emission profile more resembles the pure triplet case since the DPA triplets are now able to find a reaction partner.

since triplets that are formed have a low probability of encountering each other and a high probability of being quenched by radical ions. Simulations[25] of ECL for this system yield curves that can be used to construct a plot qualitatively similar to that in Figure 3 for the $NPK^{\bullet-}$/$DPA^{\bullet+}$ system (data not shown).

Discussion

The results of this work clearly show that electrogenerated chemiluminescence can be obtained from 9,10-diphenylanthracene through the S-route with a variety of reagents that react with DPA radical ions to produce sufficient energy for direct singlet production, consistent with previous reports.[13,14] More importantly, the results show that the T-route, a pathway followed with less energetic reagents, is surprisingly efficient. The major loss for this pathway is the quenching of triplet states by radical ions present near the reaction zone. The two different pathways can be experimentally distinguished by their reaction orders as well as the time course of ECL generation. For systems that do not produce sufficient energy to directly form the excited state, second-order behavior is observed with respect to DPA concentration and the time course of light evolution during the potential step continues to evolve, indicative of the slower kinetics of the T-route. In the case of reactants with intermediate energetics, both pathways can occur simultaneously. These findings provide strong experimental support for the mechanistic framework described in the introduction, and allow the effects of the relative reaction rates to be evaluated.

High-speed ECL generation in the flow injection system is an efficient way to rapidly examine the mechanisms that are involved in these light-producing chemical reactions.[26] The use of rapid potential steps provides less opportunity for the electrogenerated reagents to diffuse far from the electrode surface and undergo side reactions with impurities, thus simplifying mechanistic interpretation. In addition, the system facilitates the rapid survey of a series of donors and acceptors and allows study of these ECL reactions with concentrations down to the nanomolar range with energy-sufficient systems. An unidentified source of luminescence (10^3 CPS), apparently emission from an adsorbed species, prevents observation of subnanomolar DPA concentrations.

(23) (a) Hirayama, S.; Lampert, R. A.; Phillips, D. *J. Chem. Soc., Faraday Trans.* **1985**, *81*, 371−382. (b) Heinrich, G.; Schoof, S.; Gusten, H. *J. Photochem.* **1974**, *3*, 315−320.

(24) (a) Kimura, K.; Yamada, H.; Tsubomura, H. *J. Chem. Phys.* **1968**, *48*, 440−444. (b) Barah-Tosh, S.; Chattopadhyay, S. K.; Das, P. K. *J. Phys. Chem.* **1984**, *88*, 1404−1408.

(25) Similar time courses of light emission as the experimental curves could be simulated with the following parameters: $k_t = 10^{10}$ M^{-1} s^{-1}, $k_s = 10^7$ M^{-1} s^{-1}, $k_{tta} = 2 \times 10^9$ M^{-1} s^{-1}, $k_q = 10^{10}$ M^{-1} s^{-1}. Furthermore, the slope of the light emission versus DPA concentration from these simulations was noninterger like the curve shown for NPK in Figure 3.

(26) Collinson, M. M.; Pastore, P.; Maness, K. M.; Wightman, R. M. *J. Am. Chem. Soc.* **1994**, *116*, 4095−4096.

The distinction between the S- and T-routes has been previously investigated in a variety of ways. The triplet pathway has been inferred for some systems by the observation that triplet quenchers decrease photon emission.[2] The sensitivity of photon emission to magnetic fields has also been examined since this can decrease the rate of triplet quenching by radical ions.[16,27] For example, the ECL from rubrene, in which it serves as both A and D, is enhanced by magnetic fields at room temperature. In contrast, luminescence from the $DPA^{+/-}$ system is independent of magnetic field strength.[27] The two pathways have also been distinguished on the basis of their differing time courses of light generation and can be similarly distinguished by differing slopes of the data plotted in logarithmic fashion.[12] However, this approach can be problematic since side reactions, the cell time constant, and solution resistance can also affect the temporal profile. In the approach taken in this work, variation of the concentration of the limiting reactant while working at a constant frequency, all of these effects are similarly maintained over the entire range of investigation. This simplifies simulation of the reactions by reducing the number of adjustable parameters. Because only modest frequencies were employed, a microband electrode could be used, resulting in much larger photon fluxes than seen with a microdisk.

The composite plot in Figure 3 reveals in a general way that the efficiency of light production increases with the energy difference between the reacting partners. The rate constants that dictate these efficiencies (reaction 3) are determined by the sequential formation of an encounter complex that occurs under diffusion control followed by electron transfer.[5] The outer-sphere, electron-transfer reaction in the encounter complex can be predicted with Marcus theory, which states that the activation energy is a function of the free energy (ΔG_{et}) of the reaction which is linearly related to the difference in half-wave potentials of the two couples ($\Delta E_{1/2}$).[3] Not only will energetically insufficient reactions be kinetically slow, but also those with very large energetic driving forces will be as well due to the Marcus inverted region. Thus, the energetics directly dictate not only the pathway but also the efficiency. This theoretical framework predicts that the combined singlet−triplet mechanisms can occur in parallel for couples with intermediate reaction energies. The experimental results with the $NPK^{\bullet-}/DPA^{\bullet+}$ system provide the first demonstration that this is the case. Because of quenching of triplets by the radical ions that are themselves the precursors to ECL,[2,28] the simultaneous occurrence of both pathways will only be apparent for reaction partners with energy differences similar to that of the excited state singlet.

Finite difference simulations of the S- and T-routes and the agreement with experimental data further confirm the validity of the assigned mechanisms and provide the magnitude of the rate constants. For both systems, it was found that the location where the radical ions react remains essentially stationary during the reaction when unequal concentrations are used as in this work. This is because the radical ion of highest concentration reacts with the lower concentration reagent before it can leave the vicinity of the electrode. The relative position of this reaction zone to the electrode surface is dependent on the concentration of the reagents. Inspection of the computed spatial emission profiles (insert, Figure 5) for $DPA^{\bullet+}/MBP^{\bullet-}$, an S-route system, shows that increasing the concentration of the species of higher concentration moves the emission layer closer to the electrode. At close distances, energy transfer can occur resulting in greatly attenuated emission for excited singlets lying within 20 nm of the electrode surface.[26] This leads to the nonlinear curve for photon production seen in Figure 5 with high concentrations of $MBP^{\bullet-}$.

In the case of the T-route, satisfactory fits to the time course of light evolution could only be obtained when quenching of excited triplet state by radicals was included in the simulation. The photonic emission from $TMPD^{\bullet+}/DPA^{\bullet-}$ was found to exhibit a concentration-dependent reaction order with respect to TMPD, providing direct experimental evidence of quenching of triplet states by the paramagnetic radical ions. Thus, ECL generated via the energy deficient route requires a balance between the need for high radical ion concentration required to generate triplets and the quenching of these triplets by the same radical ions. The simulation results suggest that the quenching lowers the efficiency 20-fold. Thus, in the absence of quenching, the efficiency of the T-route would have approached 24%, suggesting that the statistical prediction of a probability of 1/9 for reaction 6 is an underestimate. Nevertheless, the efficiency of the T-route shown here is interesting because it is shown that relatively high yields can be obtained experimentally.

The second-order dependence of the T-route on DPA concentration, coupled with its first-order dependence of the triplet quenching reaction, dictate that systems that produce light via this pathway should be run at high DPA concentrations to maximize photonic yield. Equal concentration of both reactants or slow potential pulses under conditions of semiinfinite linear diffusion, as used in previous work,[13] are not optimal for efficient light production with the T-route. This is because those conditions allow the reaction layer to move further into the bulk of solution, which dilutes the concentration of the triplets formed via reaction 3. This has two consequences that reduce photonic emission: reaction 6 is hindered and the probability of encountering a newly generated radical ion leading to quenching is increased. However, in an electrochemical cell with two opposing electrodes such as an organic LED, the location of the reaction layer is stationary and such dilution cannot occur. Under those conditions, photon generation via the T-route could be competitive with singlet generation via the S-route. One advantage is that radical ions formed at lower potentials tend to have greater chemical stability, improving the probability that they participate in light production. Furthermore, a device operating under the T-route requires significantly lower input voltages (Table 1) than the S-route to produce photons of the same energy. Indeed, the energy gain caused by the TTA reaction is reminescent of the frequency doubling obtained with nonlinear optical materials. Thus, the results of this work suggest that T-route systems operated under optimal conditions are an attractive candidate to form practical display devices.

Acknowledgment. This research was supported by the National Science Foundation (CHE).

JA971537O

(27) Faulkner, L. R.; Tachikawa, H.; Bard, A. J. *J. Am. Chem. Soc.* **1972**, *94*, 691−699.

(28) (a) Wilkinson, F.; McGarvey, D. J.; Olea, A. F. *J. Phys. Chem.* **1994**, *98*, 3762−3769. (b) McLean, A. J.; Rodgers, M. A. J. *J. Am. Chem. Soc.* **1993**, *115*, 4786−4792. (c) Michel-Beyerle, M. E.; Kruger, H. W.; Haberkorn, R.; Seidlitz, H. *Chem. Phys.* **1979**, *42*, 441−447.